Simulation of Ultra-Small MOSFETs Using a 2-D Quantum-Corrected Drift-Diffusion Model

B.A. Biegel (MRJ Inc., NASA Ames Research Center, biegel@nas.nasa.gov, 650-604-0171), C.S. Rafferty (Lucent Technologies), Z. Yu, R.W. Dutton (Stanford Univ.), M.G. Ancona (NRL)

Abstract

We describe an electronic transport model and an implementation approach that respond to the challenges of device modeling for gigascale integration. We use the density-gradient (DG) transport model, which adds tunneling and quantum smoothing of carrier density profiles to the drift-diffusion model. We present the current implementation of the DG model in PROPHET, a partial differential equation solver developed by Lucent Technologies. This implementation approach permits rapid development and enhancement of models, as well as run-time modifications and model switching. We show that even in typical bulk transport devices such as P-N diodes and BJTs, DG quantum effects can significantly modify the I-V characteristics. Quantum effects are shown to be even more significant in small, surface transport devices, such as sub-0.1μm MOSFETs. In thin-oxide MOS capacitors, we find that quantum effects may reduce gate capacitance by 25% or more. The inclusion of quantum effects in simulations dramatically improves the match between C-V simulations and measurements. Significant quantum corrections also occur in the I-V characteristics of short-channel MOSFETs due to the gate capacitance correction.

Introduction

The unrelenting down-scaling of electronic devices toward gigascale integration levels (more than 10^9 devices per chip) is causing a fundamental change from experiment-dominated development to simulation-dominated development of new electronics technology. The cost of experiments with each new technology generation is rising rapidly with the price of more advanced fabrication instruments and facilities. These instruments must provide ever more complete and precise control of all aspects of the fabrication process in order to squeeze the same functionality into a smaller area. Higher functional density is now often accomplished the same way that humans live more densely: by building up (or down) instead of out. Advanced technologies use trenches, pillars, side-walls, overlaps, stacking, and layering, to name a few space-saving gambits. But in spite of the increasing cost and complexity of fabrication, competitive pressure is intensifying to bring new technology to market faster and cheaper than ever before. Preventing these two realities from colliding is the essence of the gigascale challenge.

In a circular process, the fundamental change in electronics R&D is made possible by the very technology that requires it. Larger, faster, and cheaper computers don't just make it possible to solve larger problems faster - they actually make it feasible to solve new classes of problems, and to solve old problems in fundamentally "smarter" ways. Thus, as experimental trial-and-error becomes infeasible in gigascale electronics development, simulation (process, device, and circuit) is becoming a fundamental part of the technology development cycle, and will eventually dominate it. In fact, circuit simulation has long ago replaced paper-and-pencil theory and experimental

circuit testing as the dominant means of new technology development.

However, meeting the gigascale challenge is much more daunting for electronic device and process modeling. Experimental iteration (guided by experience and theory) can not continue to lead new device and process technology development into the gigascale era because of rapid changes in materials and device structures, as well as increasing complex-geometry, small-geometry, quantum, and atomistic effects. Process and device simulation must take the lead in development *because* of these new challenges, but they must also be able to *handle* them. The standard approach to process and device simulation - developing independent, and often redundant, fixed-model codes all around the world - will make process and device modeling lag the technology curve. For process and device modeling to meet their gigascale challenges and thus be able to provide critical guidance to the industry, more modular, flexible, and extensible device and process simulation codes are required.

In this work, we focus on device simulation, and describe both an approach to device simulation and a physical model which advance the effort to meet the challenges described above. The device simulation approach is to specify the transport model at a high level to a general-purpose (but highly efficient) partial differential equation (PDE) solver, in this case PROPHET[1], developed by Lucent Technologies. PROPHET then solves the model in 1-D, 2-D, or 3-D for a specified device and test regime. This approach allows for the rapid investigation of a wide range of device structures, transport models and physical effects, which is essential for device simulation to play a leading role in the future of electronic device technology. [Note that the PDE solver approach is also applicable to process modeling. In fact, PROPHET was initially developed, and is still mainly used, for process modeling.]

The electronic transport model used in this work is the density-gradient (DG) quantum correction to the drift-diffusion (DD) model.[2] This model adds tunneling and quantum smoothing of carrier density profiles to the drift-diffusion model. We note that the classical drift-diffusion model is still the most extensively used model for numerical simulation of electronic devices,[3] almost 50 years after its first description,[4] and almost 35 years after Gummel[5] first described a robust numerical solution method. The longevity of the DD model is as much a testimony to the ability of scientists to add and tune additional fitting parameters (usually through mobility models) for each successive technology generation as it is to the innate accuracy of the DD model.

However, we are in a period of even more feverish advancement of electronic devices, with new generations of technology being introduced every 2 years,[6] rather than every 3 years as predicted by recent history.[7] Further, various quantum effects will quickly increase in significance, and it is unclear how well additional fitting parameters can account for these effects. Instead, we show that the density-gradient quantum correction to the DD model can efficiently account for at least some of these effects. PROPHET offers an efficient way to explore this model and quantum effects in various electronic devices.

This work begins by describing the density-gradient model P-N junction devices, and the implementation of the DG model in PROPHET. We then describe simulation results for a P-N diode in 1-D and a bipolar junction transistor (BJT) in 2-D. Next, we reformulate the DG model for use in devices with insulators. We then compare classical and DG capacitance-voltage (C-V) curves for

1-D MOS capacitors, and current-voltage (I-V) curves for ultra-small MOSFETs in 2-D. Finally, we add ionized impurity scattering to the DG model for the first time, to improve the match between simulation and experiment. A discussion and conclusions of the work follows.

Density-Gradient Model and PROPHET

The drift-diffusion and density-gradient models of carrier transport in an electronic device can be written identically:

$$\boxed{\begin{aligned} \nabla \cdot (\varepsilon \nabla \psi) &= -\rho = -q(p - n + N_D^+ - N_A^-) \\ \frac{\partial n}{\partial t} &= \frac{\nabla \cdot \boldsymbol{J}_n}{q} = \nabla \cdot (-n\mu_n \nabla \psi_n + D_n \nabla n) \\ \frac{\partial p}{\partial t} &= -\frac{\nabla \cdot \boldsymbol{J}_p}{q} = \nabla \cdot (p\mu_p \nabla \psi_p + D_p \nabla p) \end{aligned}} \tag{1}$$

In the DD model, $\psi_n = \psi_p = \psi$, which is the classical electrostatic potential. In the DG model, the electrostatic potential has a quantum correction:

$$\boxed{\begin{aligned} &\psi_n = \psi + \psi_{qn} \qquad \psi_{qn} \equiv 2b_n\left(\frac{\nabla^2\sqrt{n}}{\sqrt{n}}\right) \qquad b_n \equiv \frac{\hbar^2}{4r_n m_n q} \\ &\psi_p = \psi + \psi_{qp} \qquad \psi_{qp} \equiv 2b_p\left(\frac{\nabla^2\sqrt{p}}{\sqrt{p}}\right) \qquad b_p \equiv \frac{\hbar^2}{4r_p m_p q} \end{aligned}} \tag{2}$$

The quantum potential correction is derived from the Schrödinger equation as a sum over all wavefunctions. Obviously, this correction can not incorporate quantum mechanics perfectly into the DD model, so r_n and r_p may be used as fitting parameters. In this work, we take $r_n = r_p = 3$, which is the high temperature limit.[8] The effect of the quantum potential is to reduce the second derivative of carrier density profiles. Therefore, abrupt changes in the carrier density (e.g., at a silicon/oxide interface) are disallowed. In general, the quantum correction acts to smooth out carrier density profiles. This is a result of continuity of the quantum wavefunction.

We now describe the implementation of the DG model in the PDE solver PROPHET. Concerning material parameters, we use mobilities of μ_n = 1500 cm^2/Vs and μ_p = 500 cm^2/Vs in (1). In (2), we take $m_n = 0.19m_o$ (light electron mass) and $m_p = 0.49m_o$ (heavy hole mass) because these values result in a good match between DG simulations and experiment. That is, these carrier masses seem to dominate the quantum potential correction in cases where straight-forward comparison with experiment is possible. The more interesting implementation issues involve the PDEs. Since PROPHET has differential operators up to second order, implementing the DG model in PROPHET requires five PDEs: the three in (1) and the two in (2). Also, the quantum potential equations in (2) are multiplied by $\sqrt{n}$ and $\sqrt{p}$ respectively to make use of existing PROPHET operators. Finally, in this work we only consider the steady-state. Thus, the DG model implemented in PROPHET is:

$$
\boxed{\begin{aligned}
\nabla \cdot (\varepsilon \nabla \psi) + q(p - n + \text{netdope}) &= 0 \\
\nabla \cdot (-n\mu_n \nabla \psi_n + D_n \nabla n) &= 0 \\
\nabla \cdot (p\mu_p \nabla \psi_p + D_p \nabla p) &= 0 \\
\sqrt{n}\psi_{qn} - 2b_n \nabla^2 \sqrt{n} &= 0 \\
\sqrt{p}\psi_{qp} + 2b_p \nabla^2 \sqrt{p} &= 0
\end{aligned}} \tag{3}
$$

where $\psi_n = \psi + \psi_{qn}$ and $\psi_p = \psi + \psi_{qp}$. This PDE model, including all coefficients, is specified in a script file which PROPHET reads and executes. For example, Figure 1 shows the DG model definition for a P-N diode or BJT (bipolar junction transistor).

In the PROPHET input script, PDE models are implemented as a series of added terms. Using term2 in Figure 1 as an example, each term is composed of a geometrical and physical operator (box_div and drift_diffusion), takes one or more fields as inputs (psi_n, electrons), is added to one or more equations (electrons), and applies only in specified regions of the device (silicon). Algebraic functions of the fields (e.g., func0) are used to set up the system of equations. The code implementing operators like drift_diffusion is provided with all of the necessary field and gradient information, and takes needed parameter values from a database maintained by PROPHET. The database also stores (for a single run or permanently) the transport models.

Results: Bipolar Devices

Using the DG model described above, we consider the effects of the quantum potential on bipolar device operation. In particular, we simulate the operation of a P-N diode in 1-D and a BJT in 2-D, and compare simulation results from the classical and DG models. For the PN diode, a noticeable difference in the carrier density profiles occurs near the junction due to the profile smoothing

```
system name=dens_grad
+   sysvars=psi,electrons,holes,psi_qn,psi_qp
+   nterm=10
+   term0=box_div.lapflux(psi|psi)@{silicon}
+   term1=nodal.potflux(electrons,holes,netdope|psi)@{silicon}
+   term2=box_div.drift_diffusion(psi_n,electrons|electrons)@{silicon}
+   term3=box_div.drift_diffusion(psi_p,holes|holes)@{silicon}
+   term4=nodal.prod(psi_qn,sqrt_n|psi_qn)@{silicon}
+   term5=box_div.lapflux(sqrt_n|psi_qn)@{silicon}
+   term6=nodal.prod(psi_qp,sqrt_p|psi_qp)@{silicon}
+   term7=-1*box_div.lapflux(sqrt_p|psi_qp)@{silicon}
+   term8=dirichlet.device_dirichlet(netdope|psi,electrons,holes)@{silicon/anode,
silicon/cathode,silicon/emitter,silicon/base,silicon/base2,silicon/collector}
+   term9=dirichlet.default_dirichlet(0|psi_qp,psi_qn)@{silicon/anode,
silicon/cathode,silicon/emitter,silicon/base,silicon/base2,silicon/collector}
+   tmpvars=psi_n,psi_p,sqrt_n,sqrt_p
+   nfunc=4
+   func0=add(psi,psi_qn|psi_n)@{silicon}
+   func1=add(psi,psi_qp|psi_p)@{silicon}
+   func2=sqrt(electrons|sqrt_n)@{silicon}
+   func3=sqrt(holes|sqrt_p)@{silicon}
```

Figure 1: DG model definition for a PN diode and BJT in PROPHET script file. Associated model parameter values, domain definition, and simulation commands are not shown.

effect of the DG model. Also, note that the lower effective mass of the electrons results in a larger quantum correction (density smoothing). However, the I-V curves for the two models are indistinguishable over the entire bias range, as shown in Figure 3. [Note that (Esaki) tunneling has been neglected in these simulations, although it could in principle be included in the DG calculation.]

For the 2-D BJT shown in Figure 4, quantum effects were more noticeable in the terminal characteristics. In particular, although the currents appear to be almost identical, on average the DG collector current is roughly 5% less than the classical collector current, and the DG base current is 20% less than the classical current. These differences result in a substantial 15% *increase* in current gain with the DG quantum correction. The root cause of these I-V differences is being investigated. It does not appear to be due to a lowering of the base barrier to collector-emitter current, since collector current decreased slightly in the DG model. Solution error due to inadequate grid resolution also seems unlikely, as the result was consistent over a wide range of biases. [To avoid grid error, we used over 10,000 grid points for this simulation, mostly to adequately resolve the fairly abrupt and important base-emitter junction. As a result, this was the most computationally demanding simulation in this work.] These BJT simulation results indicate that even bulk transport devices using P-N homojunctions (rather than heterojunctions) to define regions can show significant quantum effects in their terminal (I-V) characteristics. Even more interesting is that the quantum correction actually *improved* device performance.

Density-Gradient Model with Insulators

The remainder of this work describes the implementation and use of the density-gradient model for simulation of MOSFETs.[9] In comparison to bulk-transport devices such as the P-N diode and BJT, surface transport devices such as the MOSFET demonstrate significant quantum effects. This is not surprising, since quantum effects are most prominent in the same region of the MOSFET that transport takes place: at the silicon/gate-oxide interface. Figure 7 and Figure 8 depict

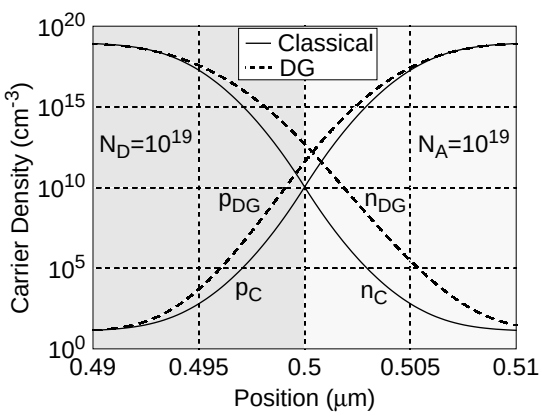

Figure 2: DG and classical carrier density profiles for a P-N diode at zero bias. The diode is 1 μm long, with $N_D = N_A = 1e19/cm^3$ on each side of the abrupt P-N junction at x = 0.5 μm. The DG quantum correction smooths carrier density profiles.

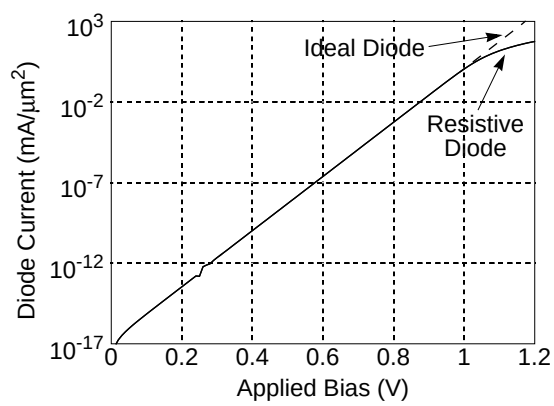

Figure 3: DG and classical I-V curves for P-N diode. The curves are indistinguishable, indicating that quantum effects do not affect the terminal characteristics of this device. The resistive region of operation is indicated.

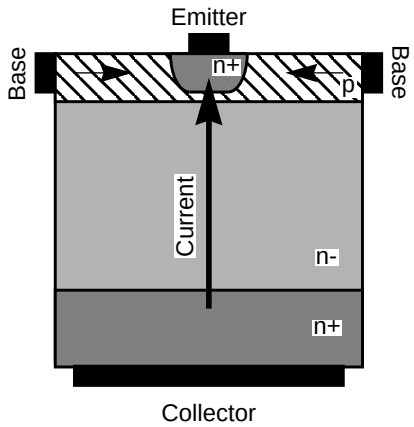

Figure 4: Simulated 2-D Silicon BJT structure (5µm square, 0.1µm base width). Note that PROPHET allows contacts along any edge of the simulation region.

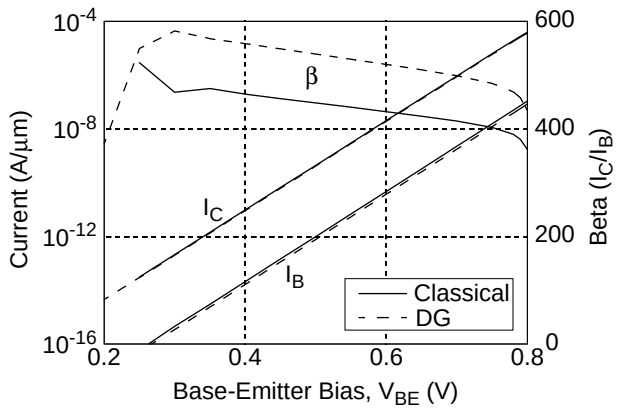

Figure 5: Collector current, base current, and current gain versus base-emitter voltage. DG base current is lower than classical base current, resulting in higher current gain in the DG model.

qualitatively the expected difference in carrier density profiles of a MOSFET operating classically and one including quantum effects. Classical carrier densities change abruptly at the oxide interfaces from some large external value to zero in the oxide. Quantum mechanically, carrier densities can not change abruptly: the densities must go smoothly to zero as it approaches the oxide interfaces. The quantum potentials of the DG model accomplish this profile smoothing, and so are largest near the oxide interfaces. Clearly, including the quantum corrections in MOSFET simulations is important. It is also somewhat more challenging than the implementation for bulk devices.

The difficulty in implementing the DG model for MOSFETs lies in formulating a reasonable boundary condition (BC) for the quantum potentials ψ_{qn} and ψ_{qp} at the oxide interfaces. To minimize computation time, we assume that in the oxide, $n = p = \psi_{qn} = \psi_{qp} = 0$, so only the

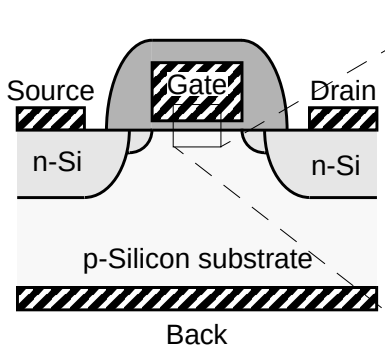

Figure 6: Basic MOSFET structure to be simulated. The poly-gate/oxide/silicon region is depicted in detail in the following.

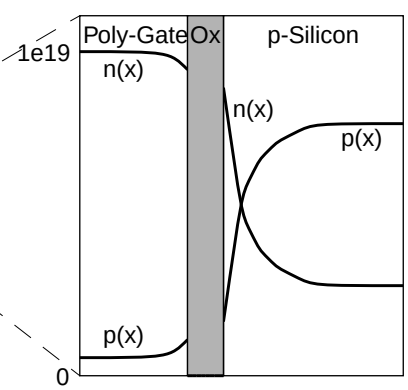

Figure 7: Classical carrier density profiles of a MOSFET in inversion. Densities are discontinuous at the oxide interface.

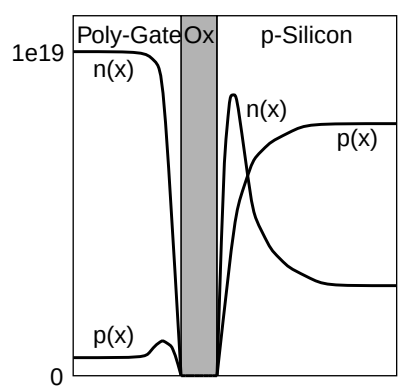

Figure 8: Quantum carrier density profiles of a MOSFET in inversion. Density discontinuities are removed by the quantum potential.

source-less Poisson equation is solved in this region. Further, due to quantum continuity of the carrier density profile, we can use $n = p \approx 0$ as BCs at the oxide interfaces. However, the quantum potentials have a relatively large, unknown value at the interfaces, since this is where they act to force electron and hole concentration to (near) zero. In other words, a Dirichlet BC can not be applied to the quantum potentials at the oxide interfaces. By the same reasoning, enforcing a Neumann BC on their gradients is also not possible. One solution to this dilemma is to solve the entire five-PDE model in the oxide as well as in the adjoining silicon and poly gate. In this case, the discontinuity in the quantum potentials would be determined by (2) and the silicon-oxide band offsets. A model implementing this approach is being developed.

Another solution to the boundary condition challenge is to use the quasi-Fermi (QF) model[10] of carrier transport, which can be described as a change of variables from the DD model. Recall that at the interface between a semiconductor and an insulator, the electron and hole quasi-Fermi levels in the semiconductor have zero gradient perpendicular to the interface (i.e., there is no current flow into the insulator). The DG equivalent of the QF model can use these Neumann BC as the constraints needed for the quantum potential PDEs. However, the PDEs must be rewritten in terms of the QF levels. The final result is:

$$\boxed{\begin{aligned} \nabla \cdot (\varepsilon \nabla \psi) + q(p - n + N_D^+ - N_A^-) &= 0 \\ -\nabla \cdot (n\mu_n \nabla \phi_n) &= 0 \\ \nabla \cdot (p\mu_p \nabla \phi_p) &= 0 \\ \sqrt{n}\psi_{qn} - 2b_n \nabla^2 \sqrt{n} &= 0 \\ \sqrt{p}\psi_{qp} + 2b_p \nabla^2 \sqrt{p} &= 0 \end{aligned}} \tag{4}$$

where the five solution variables are ψ, ϕ_n, ϕ_p, $\sqrt{n}$, $\sqrt{p}$, respectively, and the following are computed as “elimination variables”:

$$\boxed{\begin{aligned} n &= (\sqrt{n})^2 \\ p &= (\sqrt{p})^2 \\ \psi_{qn} &= \phi_n + (kT/q)\ln(n/n_i) - \psi \\ \psi_{qp} &= \phi_p - (kT/q)\ln(p/n_i) - \psi \end{aligned}} \tag{5}$$

The above QF version of the DG model was implemented in PROPHET, and is used for all of the remaining simulations in this work.

Results: Thin Oxide MOS Capacitors

The switching efficiency of a MOSFET is largely determined by its gate capacitance, which ideally measures the ability of the gate electrode to control the carrier density and current flow below the gate oxide (see Figure 6). Thus, it is critical for simulations to accurately predict gate capacitance. The quantum repulsion of carriers from both oxide interfaces, as depicted in Figure 8, makes the oxide appear to be typically 1 nm thicker than it is. This may not seem like a large amount, but real gate oxide thicknesses have already dropped below 5 nm, and are predicted to

reach 1 nm by 2012.[11] Thus, this quantum effect should already be noticeable in state-of-the-art technology, and will quickly become more so as gate oxide thicknesses continue to diminish.

To test this prediction, 1-D MOS capacitors with oxide thicknesses from 21Å to 80Å were simulated, and C-V curves were compared to those from classical simulations and from experimental measurements of the same structure.[12] The resulting carrier density profiles were as predicted in Figure 8: zero at the oxide interfaces, with the inversion or accumulation charge peak 5Å to 15Å beneath the Si-oxide interface, rather than exactly at the interface as in the classical model. Figure 9 compares C-V curves (capacitance versus gate-substrate bias V_{GS}) for the 21Å oxide MOS capacitor. As expected, the DG model reproduces measured data much more accurately than the classical model for this very thin oxide. To summarize the results of the C-V simulations over oxide thickness, Figure 10 shows the fractional error in simulated capacitance (compared to measured data) versus oxide thickness for the classical and DG models. To simplify the plot, a single bias of V_{GS} = -2V (accumulation) was chosen, since this condition is most critically affected by quantum effects and is least affected by other unknown parameters such as the poly doping level.[1] Here we see that the DG model maintains accuracy at least down to 21 Å, while the accuracy of the classical model deteriorates rapidly for oxide thicknesses below 40Å.

Results: Short Channel MOSFETs

Although 1-D simulations such as those above can provide some rough measures of device operation, the ability to perform simulations of MOSFET in at least 2-D is essential for practical application. Only with 2-D simulation can a detailed picture of operating characteristics be obtained. Of course, classical models have been used in 2-D and 3-D for many years. Quantum models based on non-equilibrium Green's functions, Wigner functions, or the density matrix can include scattering, and therefore could serve as a basis for conventional electronic device modeling including quantum effects. However, extending any of these quantum models even to 2-D will

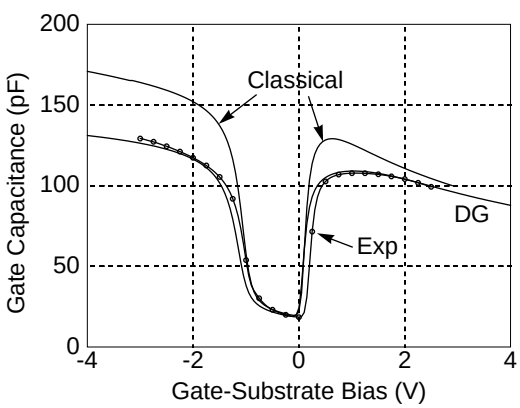

Figure 9: MOS Capacitor low frequency C-V curve comparison for (100 μm)^2 area, 21Å thick oxide. The DG model reproduces measurements (dotted curve; data courtesy of H-P Labs) much more closely than the classical model.

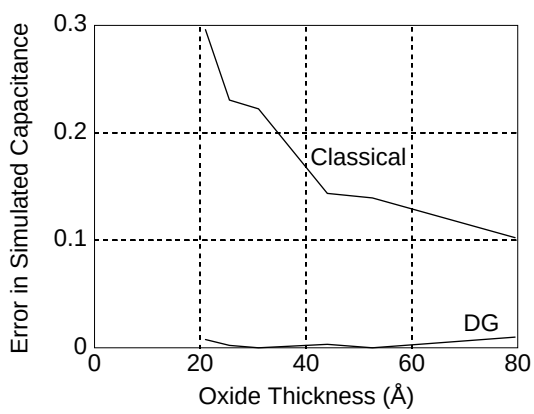

Figure 10: Fractional error in simulated capacitance versus gate oxide thickness at V_{GS} = -2V (accumulation). The DG model maintains accuracy at least down to 21 Å. The accuracy of the classical model deteriorates rapidly below 40Å.

require huge computational resources. By contrast, the DG model, with its quantum corrections, is only moderately more computationally demanding than the associated DD and QF classical models. Thus, it can also be feasibly solved in 2-D (and even 3-D). Our recent work[1] was the first to accomplish this. Here we extend those results to more detailed and complete simulations.

Figure 11 shows the simulated drain characteristic (drain current versus drain bias at a series of gate biases) for a 30 nm MOSFET with 20Å gate oxide. This device should approximate the state of the art in research labs. Computed drain characteristics for both the quantum-corrected DG model and the classical quasi-Fermi model are shown. At each gate bias, the DG current is typically 40% below that predicted by the classical model. This represents a serious decrease in the current drive capability of the device.

One question which needs to be answered is what fraction of the reduced current drive is due to the reduction in channel charge, and what fraction to quantum transport effects along the channel. Figure 12 compares the reduction in channel charge and drain current in the DG model at full drain bias (1V) for the 30 nm MOSFET simulated in Figure 11. The close match between these curves over the full range of gate biases indicates that the DG current reduction is dominated by reduced channel charge, with only minor quantum transport effects. It makes sense that quantum effects are minor in the transport direction in the DG model, since this model only significantly affects the potential and carrier profiles near abrupt heterojunctions and insulating interfaces. The relatively smooth potential in the transport direction results in small quantum potentials in this direction, and correspondingly small quantum effects on current. Note that this analysis only applies to the DG quantum model. Quantum models which include the effect of discrete quantum energy levels in the channel may predict very significant quantum transport effects in the channel.

Even though, in the industrial sense, the DG model currently implemented in PROPHET is not very sophisticated, it is instructive to compare its simulation results with measured I-V data, just

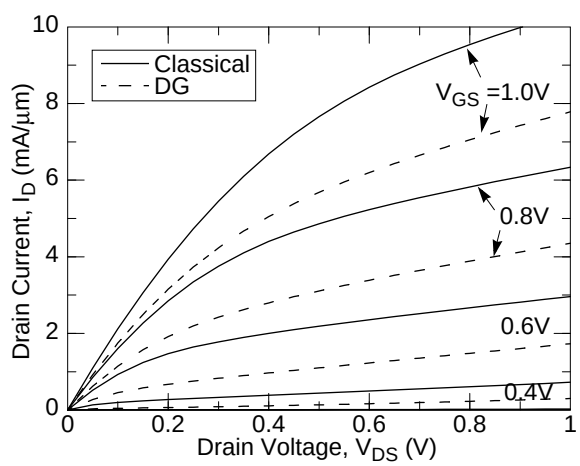

Figure 11: Computed drain characteristics for 30 nm gate length, 20Å gate oxide MOSFET. Results for classical and DG simulations are shown for $0.4V \leq V_{GS} \leq 1V$. The classical current is 25-60% larger.

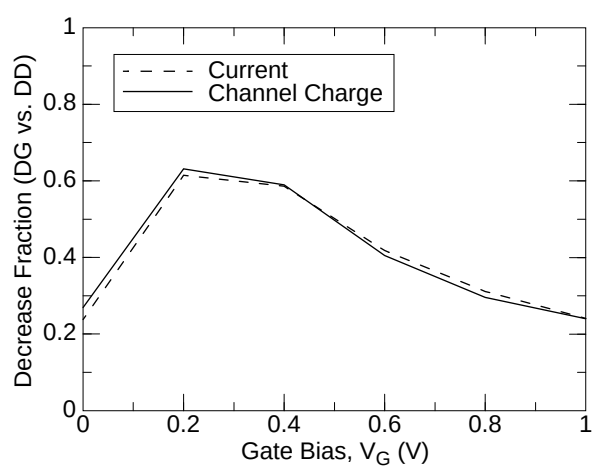

Figure 12: Reduction in current and channel charge (at mid channel with V_{DS} = 1V) in DG vs. classical model. DG current drop is dominated by reduced channel charge, with only minor quantum transport effects.

as we compared to measured C-V data. I-V measurements and doping data are not yet available for devices as aggressive as the 30 nm MOSFET simulated above. To compare to measurements, we therefore use published data from 1996 for a much larger, 80 nm MOSFET.[13] Figure 13 shows the simulated current for the DG and classical models, and Figure 14 shows the measured data for this device. We note that the reduction in current of the DG model is not nearly as severe as in the 30 nm device. More importantly, the simulated currents are about a factor of 15 larger than the measured results. We discuss this briefly in the final section.

Discussion and Conclusions

Up to this point, we have presented many simulation results using the density-gradient model, and have demonstrated both the importance and feasibility of including quantum effects in 2-D electronic device simulation. However, we promised to espouse not only a *model* suitable for meeting the gigascale challenge, but also an *approach* for implementing that model. We have discussed this approach only briefly, so we use this section to provide further detail.

There is a continuum of possible approaches to developing device modeling capability, from writing every byte of code oneself, to incorporating standard numerical libraries, to using a numerical computation package like MatLab, to using a symbolic math package like Mathematica. Ideally, the device modeling researcher seeks the shortest path between formulation of the model and analysis of device simulation results. Further, this path must remain short even as the model is modified and enhanced many times, and even if several different models are employed. This objective is *not* the same as requiring that the device modeling code run as fast as possible, since far more time is spent programming, debugging, and tuning code than running it. It is the sum of the unproductive tasks - discretizing the model, programming and debugging, and running simulations - that we seek to minimize. A tool like Mathematica appears to offer the hope of a consistently short path, freeing the model developer from writing any code and from the often difficult

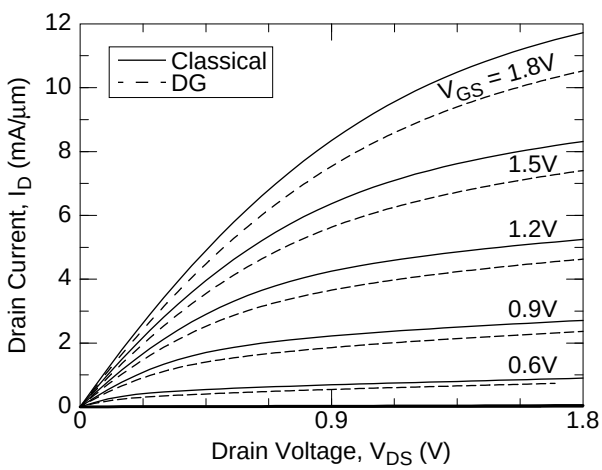

Figure 13: Computed drain characteristic for 80 nm gate length, 35Å gate oxide MOSFET. DG current is only about 10% less than classical current.

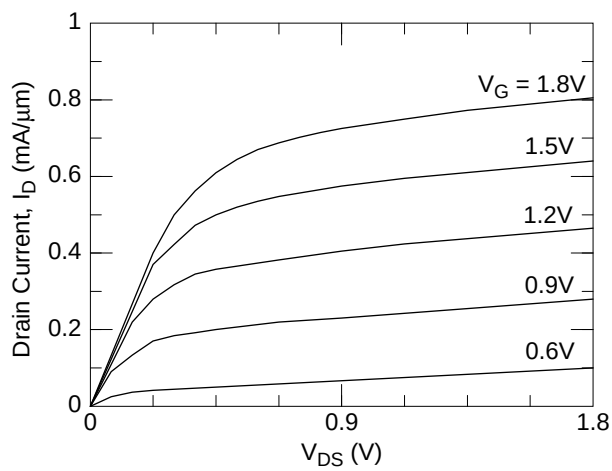

Figure 14: Published drain characteristic for 80 nm MOSFET.[13] Current is 15 times smaller and short channel effects are much less severe than in simulated results.

task of discretizing the model. However, it seems that only hand-written code offers the computational scalability, complex domains, and boundary conditions needed for “real” device modeling.

Based on our experience, PROPHET represents the kind of tool needed to minimize the unproductive part of device modeling research. PROPHET allows one to specify the transport model as a set of PDEs, so it does not require discretization, and it has a growing set of mathematical operators from which to build the PDE terms. Models which can be posed in terms of existing operators require no code to be written, while models with more complicated or unusual PDE terms will require one or more short operator routines to be created (by copying and modifying an existing operator routine). For example, all of the operators necessary to produce the drift-diffusion version of the DG model (see Figure 1) are included in PROPHET’s standard set. Three existing operators were modified slightly for the quasiFermi version of the DG model. Thus, the results of this work are the product of a very short path from model formulation to analysis.

To illustrate the development process with PROPHET, consider the issue left hanging at the end of the last section. We found that the simulated current density of the DG and classical models was about 15 times larger than measured data (Figure 13). In all of our DG simulations to date, we have used constant, intrinsic mobilities. In reality, many scattering effects combine to reduce the effective mobility by a factor of 10 or more. As a proof-of-concept, we implemented a position-dependent mobility model for ionized impurity scattering. A mobility model was selected:[14]

$$\boxed{\mu_I = \mu_{\min} + \frac{\mu_0 - \mu_{\min}}{1 + (N/N_{\mathrm{ref}})^{\alpha}}} \tag{6}$$

with different parameters $(\mu_0, \mu_{\min}, N_{\mathrm{ref}}, \alpha)$ for electrons and holes. An operator function implementing (6) was created in a few minutes. The quasiFermi and quasiFermi/DG models were modified to use the new mobility operator. Statements like

```
dbase create name=/library/physics/silicon/electrons/mu_min sval=70*1e8
dbase create name=/library/physics/silicon/electrons/nref rval=1e17
dbase create name=/library/physics/silicon/electrons/alpha_ii rval=0.7
```

were added to the input script for the 80 nm MOSFET. Inside of an hour, we had the first results showing that ionized impurity scattering alone could reduce current by a factor of about 6, to within a factor of 2 or 3 of measured data.

Again, the main feature of PROPHET is rapid prototyping: the ability to specify and modify a model at a high level, without ever writing, debugging, or modifying the low-level gridding, discretization, data handling, and solver code. [Simple operator routines are sometimes required, however.] But script-driven modeling has other important benefits that we routinely use to produce the desired results in the shortest time. For example, simulation always begin with the solution of the simplest and most robust device model, which serves as an initial guess for a more complex model. The process continues until we reach the model of interest. In some cases we may wish to investigate a certain range of operating points. In this case, a simple, fast-solving model is used to step the device into the operating region of interest, at which point the full model is engaged. In some cases, over several system solves, we gradually switch on a PDE term which renders the solution divergent if switched on abruptly.

As the cost of computation continues to decline rapidly, the overhead of using general purpose code is becoming negligible in comparison to the time it takes to write highly tuned code. This disparity in time cost will increasingly favor the use of general functionality packages such as PROPHET over writing code. The very computers we are creating will eventually make obsolete the traditional approach to electronic device modeling of spending years writing highly tuned, monolithic, "vertical" simulation codes (which only implement a single physical model). That approach will inevitably fall behind the capabilities of more general and extensible codes which allow the researcher to focus on theory and analysis, rather than programming and debugging.

In summary, we presented the density-gradient as a computationally efficient means of including quantum effects in multi-dimensional electronic device simulation suitable for gigascale integration technology. We have also presented the PDE solver PROPHET as a device modeling platform which enables rapid prototyping and enhancement of models with a level of flexibility that will be required for device modeling to provide timely guidance to the semiconductor industry in the gigascale era. We have demonstrated the robustness of this model for simulation of both bipolar and MOSFET devices. In first-ever BJT simulations, the DG model predicted an unexpected increase in the current gain. In MOS capacitor simulations, we showed that the classical model rapidly diverges from measured results for oxide thicknesses below 40 Å, while the DG model maintains good accuracy at least down to 21 Å. We found that in ultra-small MOSFET simulations, the current reductions predicted by the DG model were entirely due to the reduced inversion charge, while lateral quantum transport effects were minimal. Finally, we described the first ever DG simulations with a position-dependent mobility including ionized impurity scattering.

References

1. C. S. Rafferty, B. Biegel, Z. Yu, M.G. Ancona, J. Bude, R.W. Dutton, Proceedings SISPAD'98, Leuven, Belgium, Sept. 2-4, 1998 p. 137.
2. M.G. Ancona, Phys. Rev. B **35**, 7959 (1987).
3. E. Wang, Second NASA Device Modeling Workshop, Moffett Field, CA, Aug. 7-8, 1997.
4. W. Shockley, Bell Sys. Tech. Journal, **28**, 435 (1949). W. van Roosbroeck, Bell Sys. Tech. Journal, **29**, 560 (1950).
5. H.K. Gummel, IEEE Trans. Elec. Devices, **ED-11**, 455 (1964).
6. National Technology Roadmap for Semiconductors, p. 13 (1997).
7. G. Larrabee and P. Chatterjee, Semiconductor International, May 1991, p. 84. C. Hu, Semiconductor International, June 1994, p. 105.
8. F. Perrot, Phys. Rev. **A20**, 586 (1979). M.G. Ancona and G.J. Iafrate, Phys. Rev. **B39**, 9536 (1989).
9. M.G. Ancona, Z. Yu, W.-C. Lee, R.W. Dutton, and P.V. Voorde, J. of Technology Computer Aided Design (JTCAD), 1998 (http://tcad. stanford.edu/tcad-journal/archive).
10. S.M. Sze, "Physics of Semiconductor Devices, 2nd Ed., p. 84, Wiley, 1981.
11. National Technology Roadmap for Semiconductors, p. 46 (1997).
12. Data courtesy of Hewlett-Packard Labs, Palo Alto. Capacitor areas were $(100\ \mu m)^2$.
13. L. Su, et al., 1996 Symposium on VLSI Tech., p. 12.
14. S. Selberherr, *Analysis and Simulation of Semiconductor Devices*, p. 86, Springer-Verlag, New York, 1984.